Appl Biochem Biotechnol (2010) 160:593–603
DOI 10.1007/s12010-008-8441-7

Desulfurization of Gasoline using Molecularly Imprinted Chitosan as Selective Adsorbents

Yonghui Chang · Lei Zhang · Hanjie Ying · Zhenjiang Li · Hao Lv · Pingkai Ouyang

Received: 6 March 2008 / Accepted: 11 November 2008 /
Published online: 3 December 2008

Abstract For desulfurization of gasoline, novel chitosan-based molecularly imprinted polymer (MIP) was prepared by cross-linking chitosan with epichlorohydrin in the presence of dibenzothiophene (DBT) as the template. The influence of cross-linking ratio on the specific adsorption was evaluated. The effects of the types and the amounts of porogen on selectivity of the chitosan MIP were also examined. Results showed that MIP has a higher recognition property to DBT. The maximum rebinding capacities of the MIP reached 22.69 mg g^{-1} in the model solution. The adsorption behaviors of the MIP including adsorption kinetics, isotherms, and thermodynamic parameters were investigated and the experimental data agreed well with the Langmuir model. The dynamical adsorption behaved in first-order kinetics. Negative values for the Gibbs free energy showed that the adsorptions were spontaneous processes. The MIP was further used to selectively adsorb organosulfur from gasoline.

Keywords Molecularly imprinted polymer · Molecular imprinting technology · Dibenzothiophene · Desulfurization

Introduction

Dibenzothiophene (DBT) and its derivatives are important sulfur-containing compounds, which have received considerable attention in the design of molecular electronic devices and electron-transporting materials [1–3]. DBT and its derivatives are mostly found in coal tar and crude oil, and account for more than 70% of total organosulfur in gasoline, which have become a challenge in desulfurization investigations. In recent years, the serious environmental pollution has been caused by combustion of organosulfur compounds contained in the fuel. In addition, sulfur-containing compounds are also poisons for

Y. Chang · L. Zhang · H. Ying (✉) · Z. Li · H. Lv · P. Ouyang
State Key Laboratory of Materials-Oriented Chemical Engineering,
College of Life Science and Pharmaceutical Engineering,
NanJing University of Technology, Nanjing 210009, People's Republic of China
e-mail: yinghanjie@njut.edu.cn

catalysts used in automobiles. In an attempt to protect the environment, regulations were passed to decrease the sulfur level in many countries across the world [4].

The current industrial technique used to remove organosulfur from fuel is hydrodesulfurization (HDS). But conventional HDS process is not effective in decomposing heterocyclic organosulfur compounds, such as DBT and its derivatives, particularly 4,6-dimethyldibenzothiophene (4,6-DMDBT) [5]. Furthermore, this process has high hydrogen consumption and requires severe process conditions such as high temperature and high pressure [6]. Consequently, investigations involving new deep desulfurization methods, especially under ambient conditions without the use of hydrogen, had attracted more attention.

Another attractive alternative is adsorptive desulfurization. In recent reports, new adsorbents have been used to remove the organosulfur from fuels [7–9]. A major challenge in the use of adsorptive desulfurization is the design of the adsorbent materials which can selectively adsorb the organosulfur from fuel in the presence of large excessive aromatic compounds. In recent decades, extensive studies have indicated that molecular imprinting technology can facilitate to create affinity sites towards specific molecules [10–12]. In the last few years, newly synthesized absorbents using molecular imprinting technology have been developed and applied to extract organosulfur from the model solutions [13, 14]. Recently, Aburto et al. [15] prepared DBT-imprinted polymer by using glutaraldehyde-cross-linked chitosan which show some extent of specificity recognition, however, the adsorption capacity of the molecularly imprinted polymer (MIP) was not increased. Chitosan is a natural copolymer of 2-amino-2-deoxy-b-(1,4)-D-glucopyranose and 2-acetamide-2-deoxy-b-(1,4)-D-glucopyranose, which contains a high percentage of reactive-NH_2 and-OH groups. The adsorption capacity of cross-linked chitosan depends on the type of cross-linker and the avoidance of overabundance functional groups undergoing cross-linkage [16–18].

In this study, novel MIP adsorbents using chitosan cross-linked with epichlorohydrin (ECH) were prepared and used to selectively remove DBT from gasoline. The effect of porogen and degree of cross-linking on recognition properties and adsorption capacities of the MIP were investigated. In addition, the adsorption behaviors of the MIP adsorbents including kinetics, isotherms, and thermodynamic parameters were studied as well as the specificity recognition and competitive adsorption of the MIP adsorbents. To the best of our knowledge, this is the first paper to report on using molecularly imprinting material in the adsorptive desulfurization of gasoline.

Experimental

Materials

DBT 99% and chitosan (30 kDa) with deacetylation content of 90 % were purchased from Acros Organics. Epichlorohydrin, glutaraldehyde (GLA), and all solvents were obtained from Beijing Chemical Reagent Factory, China.

Benzothiophene (BT) 97% and 4,6-DMDBT 98 % were purchased from Sigma and used without further purification (illustrated in Fig. 1). Toluene and dimethylbenzene, supplied by Fluka, were used to check the competitive adsorption of the MIP for aromatic compounds. Commercial gasoline samples (the total sulfur concentration 145 $\mu g\ g^{-1}$) were purchased from China National Petroleum Corporation. The model gasoline is *n*-heptane solution containing toluene (15 wt.%), dimethylbenzene (15 wt.%), and DBT (200 $\mu g\ g^{-1}$).

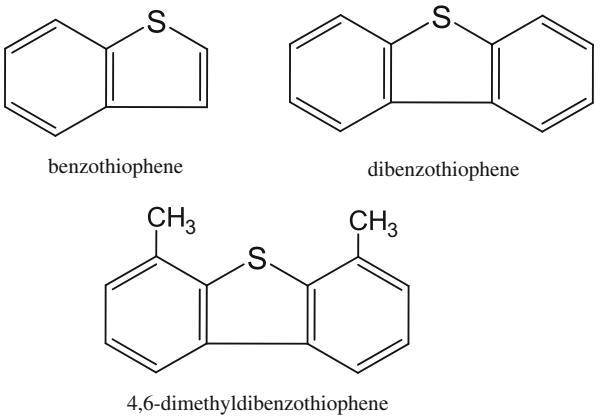

Fig. 1 Structure of major organosulphur compounds in petroleum

Preparation of Chitosan-based MIP

Two different types of chitosan-based MIP were prepared following suspension polymerization as described below.

Chitosan–ECH MIP

The imprinting phase contained chitosan (600 mg, dissolved in 30 mL of distilled water containing 2% acetic acid) and DBT (1:2.5, the molar ratio of DBT to -NH2 group in chitosan, dissolved in 4 mL of acetonitrile). The dispersing phase paraffin (60 mL) and surfactant agent Span 80 (0.5 mL) were then added. The mixture was stirred at 250 rpm for 30 min at 60 °C and the cationic amine protective agent formaldehyde (0.03 mol) was then added. The mixture was stirred for a further 30 min. Then the pH was adjusting to 10. The cross-linker ECH (0.01 mol) was added and stirred for a further 3 h at 70 °C. The chitosan–ECH MIP were collected by filtration and washed three times with petroleum ether to remove the unreacted monomers. The elimination of DBT from the chitosan-based MIP was performed by Soxhlet extraction with acetonitrile for 16 h. After drying under vacuum, the chitosan-based MIP was subjected to adsorption tests.

Chitosan–GLA MIP

The imprinting phase contained chitosan (600 mg, dissolved in 30 mL of distilled water containing 2% acetic acid) and DBT (1:2.5 the molar ratio of DBT to -CH2OH group in chitosan, dissolved in 4 mL of acetonitrile). The dispersing phase paraffin (60 mL) and surfactant agent Span 80 (0.5 mL) were then added. The mixture was stirred at 250 rpm for 30 min at 60 °C. Then the cross-linker GLA (8 mmol) was added and stirred for a further 3 h at 70 °C. The post-treatment process of chitosan–GLA MIP was carried out in same manner as that of chitosan–ECH MIP.

The preparation of the non-imprinted polymer (NIP) adsorbents followed the same procedure described above without addition of DBT.

Adsorption Test

Adsorption assays were carried out to evaluate the loading capacity and selectivity of chitosan-based MIP. Fifty milligrams of the MIP adsorbents were added to screw cap tubes

and mixed with 10 mL of *n*-heptane solution, which contained a specified concentration mixture of organosulfur and aromatic compounds. The screw cap tubes were stirred at room temperature for 12 h. After centrifugation and filtration, the resulting supernatant fluids were determined by HPLC (Beckman, USA, 166 detector, 207 LC pump, 508 auto injector) at 232 nm using a C18 ODS reverse phase column. The HPLC conditions were as follows. Methanol containing 25 % of redistilled water (*v*/*v*) was used as the mobile phase at a flow rate of 1.0 mL min^{-1} and the volume of liquid injected was 20 μL. The corresponding adsorption assays were also carried out using NIP adsorbents.

The static distribution coefficient K_D and imprinting factor (α) are utilized to evaluate the specific adsorption of the MIP. K_D and α are defined as

$$K_D = C_P/C_S \tag{1}$$

$$\alpha = K_{MIP}/K_{NIP} \tag{2}$$

where C_P (mg g^{-1}) is the equilibrium adsorption capacity on the MIP or the NIP and C_S (mg mL^{-1}) is the concentration of DBT in the solution at adsorption equilibrium, K_{MIP} and K_{NIP} are the static distribution coefficient of DBT on the MIP and the NIP, respectively. C_P and α are indicated as rebinding capacity and imprinting effect, respectively.

Results and Discussion

The sulfur atom in thiophene framework of DBT has a lone-pair electron. The inducement effect of sulfur atom will attract electron orientation deflection, which causes sulfur atom to possess a partial negative charge. The electron cloud density of heterocyclic group in DBT is strong to phenyl and is affected by electrophilic groups. Therefore chitosan, having mass cationic amine groups, may form an electrostatic attraction with DBT, the electrostatic attraction between the amino group in chitosan and the sulfur atom in DBT should play an important role in the selective recognition during the DBT adsorption process.

In this work, GLA and ECH were selected as convenient cross-linking agents to test the above-mentioned notion. It can be seen from Table 1 that chitosan–ECH MIP had a good imprinting effect (α=2.45) and a higher adsorption capacity (C_P= 22.69 mg g^{-1}) than chitosan–GLA MIP. Experimental results showed that the MIP adsorbents cross-linked with GLA had almost the same adsorption capacity for DBT as the NIP adsorbents.

This may be attributed to the different functional groups of chitosan reacting with the different cross-linking agents in the cross-linking reaction. An advantage of using ECH as a

Table 1 Binding specificity and imprinting effect of MIP and NIP for different cross-linker.

Sample structure	C_P (mg g^{-1})	K_D (ml g^{-1})	α
Chitosan-ECH MIP	22.69	56.73	2.45
Chitosan-ECH NIP	10.37	23.15	
Chitosan-GLA MIP	7.36	15.90	1.01
Chitosan-GLA NIP	7.29	15.71	

Adsorption of DBT: 50 mg of dried chitosan-based adsorbents incubated with 10 mL of DBT (C_0=0.5 mg mL^{-1}) at 15 for 12 h

cross-linking agent is that it not only reacted with amino groups, but also with hydroxyl groups in chitosan. While GLA only reacted with the available amino groups in the reaction, which was the major adsorption site in the DBT adsorption process. As a consequence, GLA reacted with more amino groups and reduced the number of imprinting sites for the DBT, resulting in the low adsorption amount. ECH was therefore the most suitable cross-linking agent in the preparation of DBT-MIP adsorbents.

Effect of ECH/chitosan Weight Ratio

The cross-linking ratio, the mass ratio of cross-linker to functional monomer, is a key parameter which greatly affected the rebinding capacities and imprinting effect of chitosan-based MIP to certain target molecule. In this reports, by regulating addition amount of the cross-linker, a series of experiments were performed to investigate the effect of degree of cross-linking on chitosan–ECH MIP.

It can be seen from Table 2 that for relatively low cross-linking ratios at 0.2 and 0.4, MIP had almost the same rebinding capacities as the corresponding control polymer and showed a poor recognition property.

According to experimental data, a significant imprinting effect was observed, when the cross-linking ratio was 0.8. This might also indicate that a high degree of cross-linking of the chitosan-based MIP resulted in a certain rigidity of the polymer matrix, which is important in preserving the imprinted memory and maintain specific recognition sites with the change of temperature, pH, and solvent. It is especially important to chitosan polymer, which has relatively poor mechanical properties. The cationic amine group of chitosan is the specific adsorption site which recognizes DBT. The chemical cross-linking reaction mainly takes place between the hydroxyl group of chitosan and ECH. Therefore, the increase in the cross-linking ratio would not significantly reduce available rebinding capacity.

When the cross-link ratio was greater than 0.8, the rebinding capacities of the MIP rapidly decrease along with the increase of cross-link ratio. It is possible that more functional groups were polymerized to form polymer, so that the number of specific recognition sites were reduced for imprinting molecule. Furthermore, the degree of difficulty for the DBT molecule to diffuse through the chitosan-based MIP also increased. As a compromise, an ECH/chitosan weight ratio (0.8) was selected as the optimum cross-linking ratio in subsequent experimentation.

The Effects of Porogen

The effects of porogenic agents acetonitrile, toluene, and chloroform, on the imprinting effect were assessed in this study. After testing the rebinding capacity of resulting imprinted polymers, MIP prepared in acetonitrile was more selective for DBT than in other porogens. Acetonitrile was therefore chosen as the porogen for all subsequent investigations.

Table 2 Effects of degree of cross-linking to the recognition property.

The rate of cross-linking	0.2	0.4	0.6	0.8	1.0	1.2
$C_{P,MIP}$ (mg g^{-1})	10.71	10.73	14.47	22.69	19.62	16.17
$C_{P,NIP}$ (mg g^{-1})	10.67	10.63	10.63	10.37	10.09	9.53
α	1.00	1.00	1.36	2.45	1.94	1.79

Table 3 Comparison of rebinding profile and pore structure of polymers generated by different amount of porogen.

ECH/chitosan weight ratio	C_P (mg g^{-1})	α	Surface area (m^2 g^{-1})	Pore volume (cm^3 g^{-1})
3	14.34	1.43	75	0.017
6	18.87	1.87	105	0.079
10	22.69	2.46	167	0.473
14	16.15	1.52	126	0.166

The amount of porogen was another key parameter to significantly affect the physical nature of the product, such as surface area and pore volume. The Chitosan–ECH MIP materials prepared with 0.1 to 3.0 volume ratios of acetonitrile/ECH were used to determine the effects of amount of porogen. The BET surface area and pore volume were measured by nitrogen adsorption porosimetry (Micromeritics, ASAP-2000).

Table 3 summarizes the relation between pore structure and the amount of porogen. Pore volume was found to increase as the amount of porogen increased and rebinding capacities were gradually enhance with increased consumption of porogen. The rebinding capacities reached maximum values when volume ratio of acetonitrile/ECH was 10. However, when the amount of porogen was too large, the rebinding capacities declined. This can be explained by the fact that the rigidity framework, to maintain recognition sites for the target molecule, was weakened when excessive amounts of porogen were used. Thus when solvent was extracted, the likelihood of pore structure collapse increased. MIP has a very low surface area in the dry state. In the corresponding control polymer, the same low rebinding capacities were observed.

The Kinetics of Adsorption

The kinetics of adsorption is one of the important characteristics in defining the efficiency of adsorption. Figure 2 represents the adsorption kinetics curve for DBT using the MIP at different temperature and shows that the adsorption equilibrium was achieved after 300 min for C_S. The kinetic curve for DBT showed that the adsorption was rapid for the first

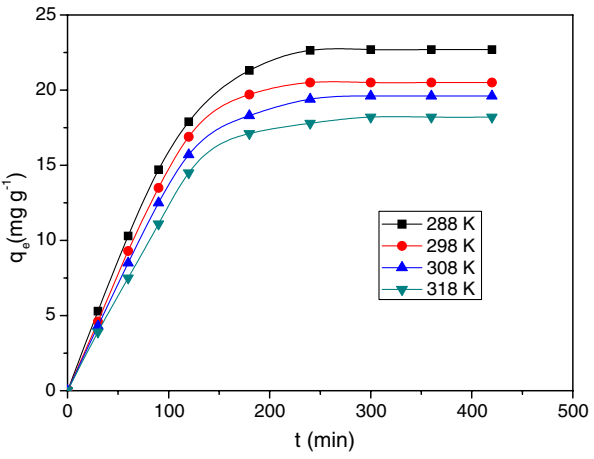

Fig. 2 Adsorption kinetics of DBT on chitosan-based MIP at different temperature

120 min and then increased slowly with time extension. Five hours later, the adsorption process reached equilibrium. In other words, the DBT adsorption is fast initially, but after the surface adsorption, the penetration of DBT molecule into the MIP becomes much more difficult.

In order to investigate the kinetic mechanism that controls the adsorption process, the pseudo-first-order (Eq. 3) and pseudo-second-order models (Eq. 4) were tested using dynamic experimental data, respectively:

$$\log(q_e - q_t) = \log q_e - \frac{k_1}{2.303} t \tag{3}$$

$$\frac{t}{q_t} = \frac{1}{k_2 q_e^2} + \frac{1}{q_e} t \tag{4}$$

where q_e and q_t (mg g^{-1}) are the amounts of DBT adsorbed on MIP at equilibrium and time t, respectively. k_1 (min^{-1}) is the pseudo-first-order adsorption rate and was calculated by plotting the $\log(q_e - q_t)$ versus t. k_2 (g mg^{-1} min^{-1}) is the adsorption rate constant of pseudo-second-order and was calculated from the slope and intercept of the plots t/q_t versus t.

The results are given in Table 4. Based on the obtained correlation coefficients (R^2), the pseudo-first-order model fitted the experimental kinetic data better than the pseudo-second-order model and conformed that adsorption rate was controlled by mass transfer in solution.

Adsorption Isotherms

Subsequently, batch adsorption experiments were conducted by placing 100 mg of MIP in 100 mL reagent bottles containing 30 mL of various concentrations of DBT solution. Figure 3 represents the adsorption isotherms curve of DBT on the MIP at different temperatures. The equilibrium adsorption behavior can be described by the Langmuir adsorption equation (Eq. 5) and the Freundlich isothermal equation (Eq. 6), respectively:

$$\frac{C_e}{q_e} = \frac{C_e}{Q_m} + \frac{K_d}{Q_m} \tag{5}$$

$$\log q_e = \frac{1}{n} \log C_e + \lg k \tag{6}$$

where q_e (mg g^{-1}) and C_e (mg mL^{-1}) are the amount adsorbed on optimized MIP and the concentration of DBT in the solution at adsorption equilibrium, Q_m is the theoretical maximum adsorption capacity at monolayer (mg g^{-1}), K_d (L mg^{-1}) is the Langmuir constant (related to the affinity of adsorption sites) and k and n are Freundlich constants

Table 4 Coefficients of pseudo-first-order, pseudo-second-order kinetic models at different temperatures.

T (K)	Pseudo-first-order kinetics		Pseudo-second-order kinetics	
	k_1 (min^{-1})	R^2	k_2 (g mg^{-1} min^{-1})	R^2
288	0.017	0.986	4.253×10^{-4}	0.919
298	0.020	0.978	4.299×10^{-4}	0.820
308	0.017	0.990	4.491×10^{-4}	0.830
318	0.018	0.981	4.440×10^{-4}	0.820

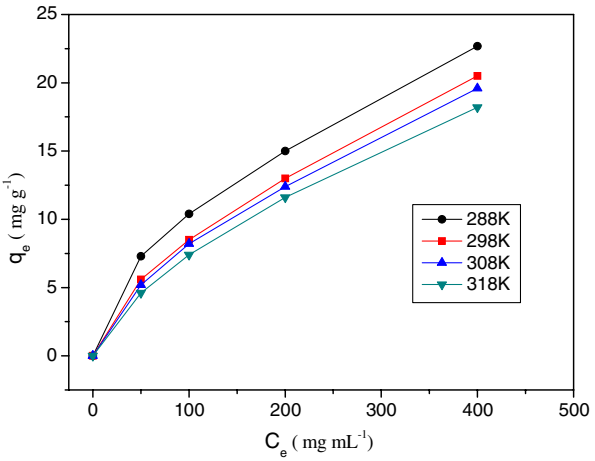

Fig. 3 Adsorption isotherms of DBT onto chitosan-based MIP at different temperature (DBT concentration, 50–400 mg/L)

indicating adsorption capacity and intensity, respectively. k and n can be determined from a linear plot of log q_e against log C_e.

The adsorption data fitted with both the Langmuir and Freundlich isotherm models are shown in Table 5. The Freundlich equation had been applied in the adsorption process using non-covalently imprinted polymers [19–21] and Langmuir equation was probably proof of predominant chemical adsorption, which may usually means monolayer adsorption on the surface of the adsorbents. In this study, the Freundlich adsorption equation fitted better (larger correlation coefficient R^2) with equilibrium data from batch adsorption experiments, which means that the adsorption of DBT on the MIP is a multiple layer adsorption.

Finally, in order to explain the effect of temperature on the adsorption thermodynamic parameters, the standard free energy $\Delta G°$, standard enthalpy $\Delta H°$, and standard entropy $\Delta S°$ were determined using the following equations, respectively:

$$\Delta G^\circ = -RT\ln K_c \tag{7}$$

$$\ln K_C = \frac{-\Delta H^\circ}{RT} + c \tag{8}$$

$$\Delta S = \frac{\Delta H^\circ - \Delta G^\circ}{T} \tag{9}$$

Table 5 Parameters of the Langmuir adsorption equation and Freundlich isothermal equation for adsorption experimental data.

T (K)	Langmuir parameters			Freundlich parameters		
	Q_m (mg g^{-1})	K_d (mg L^{-1})	R^2	k	n	R^2
288	25.64	92.89	0.858	0.987	1.938	0.999
298	24.00	116.86	0.798	0.939	2.029	0.991
308	23.25	124.66	0.777	0.930	2.062	0.989
318	21.77	126.90	0.776	0.913	2.122	0.981

Table 6 The thermodynamic parameters for the adsorption of DBT onto the chitosan-based MIP.

Temperature (K)	K_c(ml g^{-1})	$\Delta G°$ (kJ mol^{-1})	$\Delta H°$ (kJ mol^{-1})	$\Delta S°$ (J mol^{-1})
288	56.73	−9.67	5.39	52.29
298	51.25	−9.75		50.81
308	49.00	−9.97		49.87
318	45.50	−10.09		48.68

where R is the gas constant and K_c is an equilibrium constant ($K_c = C_P/C_S$). Here C_p and C_S are the equilibrium concentrations of DBT in the MIP and solution, respectively. $\Delta H°$ can be determined from a linear plot of ln K_c against 1,000/T. Table 6 shows the thermodynamic parameters. Negative $\Delta G°$ and positive $\Delta S°$ values confirm that adsorption can take place automatically. Positive $\Delta H°$ shows that the adsorption is endothermic.

Specificity Recognition and Competitive Adsorption

The recognition properties of the MIP compared to the NIP were evaluated by rebinding capacities to DBT and its structural analogue. Fifty milligrams of chitosan-based MIP synthesized under the optimized conditions was mixed with 10 mL of *n*-heptane solution known concentrations of heterocyclic organosulfur compounds (0.4 mg mL^{-1} (BT), 0.5 mg mL^{-1} (DBT), and 0.6 mg mL^{-1} (4,6-DMDBT)), respectively.

From Fig. 4, it can be seen that the chitosan-based MIP was reasonably selective for these organosulfur compounds. The corresponding non-imprinting polymer also showed moderate absorption for organosulfur compounds, but the selectivity of the non-imprinting system was less than that of the imprinting system.

Competition adsorption of aromatic compounds, which exist in concentrations of >20 wt.% in comparison with less than 1 wt.% total sulfur concentration, is a major difficulty in adsorptive desulfurization technology. Adsorption assays were carried out in the model gasoline to evaluate the competitive adsorption of aromatics. The rebinding capacity of the NIP was drastically decreased (from 11.3 mg g^{-1} to 2.1 mg g^{-1}) in contrast to the MIP system only showed a slight decrease (from 22.67 mg g^{-1} to 20.14 mg g^{-1}). It

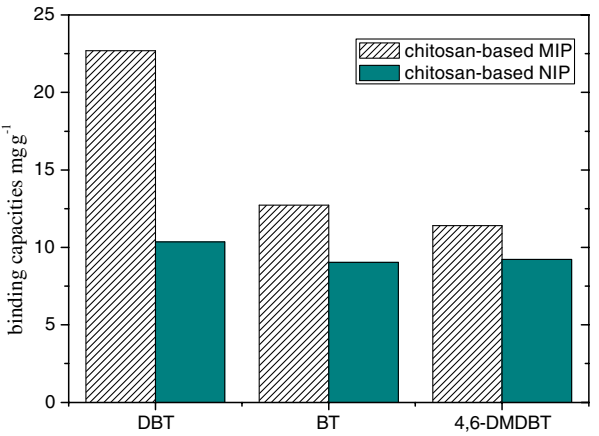

Fig. 4 Binding selectivity of MIP on different organosulphur compounds

can be explained by the fact that the adsorption of the DBT on MIP results from the imprinting effect, but non-imprinting system results from non-specific adsorption.

Adsorptive Desulfurization of Gasoline

The π-complexation method reported very recently was assessed. However, using this strategy, the aromatics strongly competed with thiophenic sulfur compounds on the surface by π-complexation. Recent studies showed adsorption capacity of Ag-exchanged Y-zeolite decreased by about 18 times when 10 wt.% of toluene (aromatic) was added to the fuel [22].

Adsorptive desulfurization assays were performed at 25 °C. Approximately 1 g of the optimum Chitosan–ECS MIP was added to 100 mL gasoline sample containing 145 μg g^{-1} sulfur together with 20 wt.% of aromatics. After mechanical agitation for 7 h, the total sulfur concentration of gasoline sample decreased to 109 μg g^{-1}. The sulfur content could be decreased to 93 μg g^{-1} by repeating three times adsorption process, The Saturated sulfur adsorption capacity of the MIP was 3.52 mg g^{-1}. After adsorption process, the Chitosan–ECS MIP was regenerated using 0.5 mol L^{-1} methanol/acetone (1/4, *v*/*v*) mixture in a thermostatic shaker at 25 °C for 6 h, The regenerated MIP adsorbents were then dried and reused in the next cycle of adsorption experiments. The adsorption capacity of imprinting microgels did not decrease after ten adsorption–regeneration cycles.

Conclusion

In this work, the chitosan-imprinting polymer was used as a highly selectivity adsorbent for sulfur compounds. The results showed that the cross-link ratio was a key parameter for the chitosan-based MIP. The effects of the type and amount of porogen to specific recognition were also evaluated. The maximum rebinding capacity of MIP was 22.69 mg g^{-1} and the imprinting effect reached 2.45. In the equilibrium studies, the experimental data fitted the Freundlich model. The pseudo first-order kinetic model agreed very well with the dynamical behavior for the adsorption of DBT on the MIP. This suggested that the adsorption of DBT onto the MIP was a multiple layer adsorption and the rate-limiting step may be the mass transport but not the chemical adsorption. Investigation on adsorption thermodynamics confirmed that the adsorption process was spontaneous nature and endothermic. These data obtained show that chitosan-imprinting technique can remove organosulfur in gasoline indirectly.

Further work is in progress to choose a functional monomer, which can form stronger complex with organic sulfur. In addition, the investigation of imprinting with other organosulfurs, such as BT and 4,6-DMDBT, is needed to achieve broader application in desulfurization. The studies in this report highlight the potential use of the MIP, as a selectivity adsorbent in desulfurization of gasoline. We expect that the molecular imprinting technique will be further applied to other oils.

Acknowledgements This work was partly supported by the Graduate Student Innovation Project of Jiansu Province (Proj. NO. xm04-45) and the Major State Basic Research Development Program of China (973 Program NO.2007CB714305).

References

1. Huang, T. H., Whang, W. T., Shen, J. Y., et al. (2006). *Advanced Functional Materials*, *16*, 1449–1456. doi:10.1002/adfm.200500823.
2. Wang, B. H., Yin, J., Xue, M. Z., et al. (2003). *Synthetic Metals*, *132*, 191–195. doi:10.1016/S0379-6779(02)00445-9.
3. Yang, W., Niu, Y., Liu, C., et al. (2003). *Synthetic Metals*, *135–136*, 183–184. doi:10.1016/S0379-6779(02)00527-1.
4. EPA, Reducing Non-road Diesel Emissions, US Environmental Protection Agency, April 2003.
5. Hou, Y. F., Kong, Y., & Yang, J. R. (2005). *Fuel*, *84*, 1975–1979. doi:10.1016/j.fuel.2005.04.004.
6. Babich, I. V., & Moulijn, J. A. (2003). *Fuel*, *82*, 607–631. doi:10.1016/S0016-2361(02)00324-1.
7. Hernandez-Maldonado, A. J., & Yang, R. T. (2004). *Industrial & Engineering Chemistry Research*, *43*, 1081–1087. doi:10.1021/ie034206v.
8. Salem, S. H., & Hamid, H. S. (1997). *Chemical Engineering & Technology*, *20*, 342–347. doi:10.1002/ceat.270200511.
9. Ma, X. L., Velu, S., Kim, J. H., et al. (2005). *Applied Catalysis B Environmental*, *56*, 137–147. doi:10.1016/j.apcatb.2004.08.013.
10. Caro, E., Marcé, R. M., & Peter, A. G. (2004). *Journal of Chromatography A*, *1047*, 175–180.
11. Hunnius, M., Rufińska, A., & Maier, W. F. (1999). *Microporous and Mesoporous Materials*, *29*, 389–403. doi:10.1016/S1387-1811(99)00008-6.
12. Weetall, H. H., & Rogers, K. R. (2004). *Talanta*, *62*, 329–335. doi:10.1016/j.talanta.2003.07.014.
13. Castro, B., Whitcombe, M. J., & Vulfson, E. N. (2001). *Analytica Chimica Acta*, *435*, 83–90. doi:10.1016/S0003-2670(01)00799-1.
14. Chang, Y. H., Liu, B., & Ying, H. J. (2003). *Ion Exchange and Adsorption*, *19*, 450–456.
15. Aburto, J., Mendez-Orozco, A., & Borgne, S. L. (2004). *Chemical Engineering and Processing*, *43*, 1587–1595. doi:10.1016/j.cep.2004.02.006.
16. Wan Ngah, W. S., Ab Ghani, S., & Kamari, A. (2005). *Bioresource Technology*, *96*, 443–450. doi:10.1016/j.biortech.2004.05.022.
17. Baroni, P., Vieira, R. S., & Meneghetti, E. (2008). *Journal of Hazardous Materials*, *152*, 1155–1163. doi:10.1016/j.jhazmat.2007.07.099.
18. Varmaa, A. J., Deshpandea, S. V., & Kennedy, J. F. (2004). *Carbohydrate Polymers*, *55*, 77–93. doi:10.1016/j.carbpol.2003.08.005.
19. Xia, Y. Q., Guo, T. Y., & Song, M. D. (2008). *Reactive & Functional Polymers*, *68*, 63–69. doi:10.1016/j.reactfunctpolym.2007.10.018.
20. Umpleby, R. J., Baxter, S. C., & Bode, M. (2001). Polymers. *Analytica Chimica Acta*, *435*, 35–42. doi:10.1016/S0003-2670(00)01211-3.
21. Wong, Y. C., Szeto, Y. S., & Cheung, W. H. (2003). *Langmuir*, *19*, 7888–7894. doi:10.1021/la030064y.
22. Velu, S., Watanabe, S., & Ma, X. (2003). *American Chemical Society Division of Petroleum Chemistry Preprints*, *48*, 56–57.